A High Efficiency Three-phase AC Motor Drive Converter that Utilized the Neutral Point of a Motor

Goh Teck Chiang
Nagaoka University of Technology
Niigata, Japan
tcgoh@stn.nagaokaut.ac.jp

Jun-ichi Itoh
Nagaoka University of Technology
Niigata, Japan
itoh@vos.nagaokaut.ac.jp

Abstract— **This paper exams a three-phase power converter that utilized the neutral point of the motor and demonstrates the motor performance of the proposed converter under various operating conditions. The structure of the proposed circuit is basically consisting of an AC/AC converter (Indirect Matrix Converter (IMC)) and a boost converter that connected to the neutral point of an induction motor. Boost converter will connect to batteries to serve as a secondary input power source of the system. Secondary input power will be injected directly into the DC link voltage of the IMC. In addition, this paper also demonstrates that the DC link voltage of the indirect matrix converter is stable and capable for an additional DC power source connection. Several motor test data such as speed-torque characteristic, torque impact and acceleration-deceleration characteristic are included to confirm the performance of the induction motor. Furthermore, experimental analysis proved that this converter is low loss when controlling with carrier comparison method of either the symmetrical method or the asymmetrical method.**

Keywords-component; Indirect Matrix Converter, Boost Converter, Induction Motor, Neutral point of the motor, Zero vector output)

I. INTRODUCTION

Hybrid electric vehicles (HEVs) is one of the promising fuel efficiency vehicles that target to occupy 20% of the total vehicle in Japan by 2020 [1]. The research in HEVs has proven that this vehicle able to reduce 48% of CO_2 compare to normal vehicles. Therefore, the known issues in HEVs are actively studying recently. These issues are such as costing, size, battery technical issues and high reliability electric motor.

The authors have proposed an AC/DC/AC circuit that applicable in a HEV system [2]. This proposed circuit greatly reduced the size of the converter by removing two passive components; electrolytic capacitors and a boost reactor, by utilizing the neutral point of the motor. In the view of the converter, the proposed circuit has successfully demonstrated the fundamental operation.

However, in the view of the motor, a study needs to analysis to confirm the stability and performance of the motor. This paper studies the performance of a 750 W induction motor that the neutral point connection is utilized by the proposed circuit. The stability and the performance of the induction motor are analyzed in an experimental. These analyses include the speed-torque curve, the torque impact characteristic and the acceleration-deceleration characteristic. In addition, these analysis are conducted in a way that modeling to a hybrid system.

II. CIRCUIT TOPOLOGY

An indirect matrix converter has shown good varieties of usages as a three-phase AC converter [3]-[4]. This converter is divided into two sides; the primary side which is a current source inverter switches at zero current and result this converter to achieve high efficiency. Furthermore, if RB-IGBTs are used in the primary side, the reverse blocking ability of the IGBT can further reduce the conduction loss in the primary side and increase the overall efficiency [5].

Besides from that, comparing an indirect matrix converter to a matrix converter, indirect matrix converter has a simple control structure because it can divided into two circuit structures but also the DC link voltage can be simply connected to other DC source. In Ref [6], this paper shows that an extra circuit is required for the connection of DC link voltage of a matrix converter. The size and cost would be increased due to the extra used components.

Fig. 1 shows the proposed circuit where it is basically constructed by an indirect matrix converter and the DC link voltage of the indirect matrix converter is connected a DC source power and a DC boost converter [2]. Furthermore, the boost converter connects to the neutral point of the motor and utilizes the leakage inductance of the motor as a boost reactor.

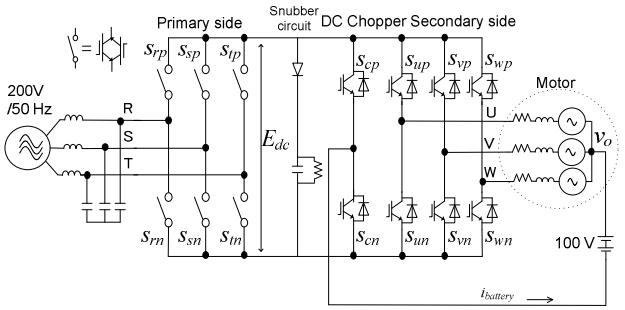

Fig.1. Proposed circuit topology.

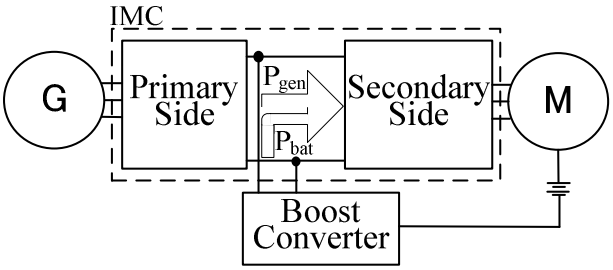

Fig. 2(a). HEV mode energy flow diagram.

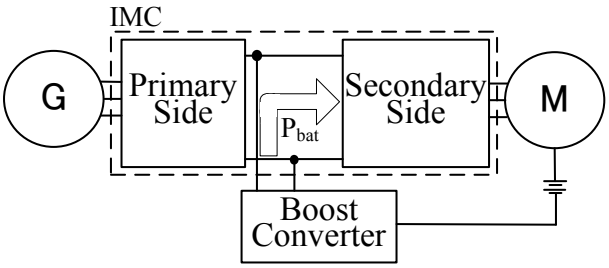

Fig. 2(b). EV mode energy flow diagram.

Fig.2. Energy flow diagram.

The boost converter operation depends on the zero vector output of the inverter side. The battery current will be charged through the motor leakage inductance at every zero vector output period. Then, the accumulated battery energy will be released into the indirect matrix converter at every non zero vector period.

In the view of a hybrid system, the proposed circuit is capable of operating in three modes. Fig. 2 illustrates the energy flow diagram of the proposed circuit. Fig. 2(a) shows the typical hybrid mode, where the battery power is used as an alternate energy to drive the motor and the main power is from the generator. Fig. 2(b) shows the EV (electric vehicle) mode operation, where all the power is drain from battery power only. The third is the normal mode, where all the input power is from generator only.

III. MOTOR CONTROL DESCRIPTION

The selection of motor for the proposed circuit is important. The motor needs to have two functions; one is the normal motoring function and regenerating function; and the second is connection point of neutral point for boost converter operation.

This paper exams and analysis the performance of a three-phase induction motor that applied in the proposed circuit. Table I shows the parameters of the induction motor and the ES servo motor. Fig. 3 demonstrates the set up condition between the induction motor and the ES servo motor. The ES servo motor is performed as a motor load. Torque sensor and speed sensor are located at the ES servo motor. The induction motor is powered by the indirect matrix converter, and the ES servo motor is directly connected to a grid power source. A controller is attached to the ES servo motor to control the torque directly. Speed and torque data can be read from the controller for the monitoring purpose.

Fig. 4 shows the control block diagram for the motor and the boost converter. This control is based on carrier comparison method [7]. First of all, V/f control could easily control a wide range of motor parameters [8]-[9]. The motor voltage is adjusted proportionally to the output frequency. Then, the magnetizing current of the motor is kept practically constant in a wide adjustment range. As a result, a constant torque can be controlled across the entire speed adjustment range.

Then the output voltage command needs to compensate with the DC link ripple which contains 6 times frequency of the input frequency. A carrier generator which will produce a variable carrier that based on the duty of the primary side, will be used in the secondary side and the chopper side. There are two types of variable carrier which is known as the symmetrical carrier and the asymmetrical carrier [2]. These two methods are formed based on the primary duty, but the symmetrical generates a 20 kHz switching frequency and the asymmetrical generates a 10 kHz switching frequency.

Boost converter controller contains of a PI control for the control of battery current and then is multiplied with the DC link frequency compensator to obtain the desired switching pattern.

TABLE I. MOTOR PARAMETERS

Induction motor (Fuji: MLH6085M)			
Motor Power	750 W	Poles	4/ 50 Hz
Rated Voltage	200 V	Rated RPM	1420
Rated Current	3.6 A	Leakage inductance	4.42 mH
ES Servo motor (Fuji: GRK1151A)			
Motor Power	1500 W	Rated RPM	2000
Rated Votlage	200 V	Rated Torque	7.16 N.m
Rated Current	8.6 A	Max Torque	10.8 N.m

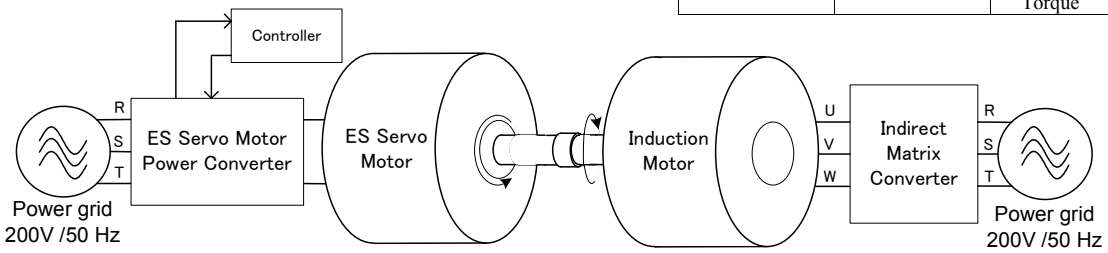

Fig. 3. Motor experimental set-up condition.

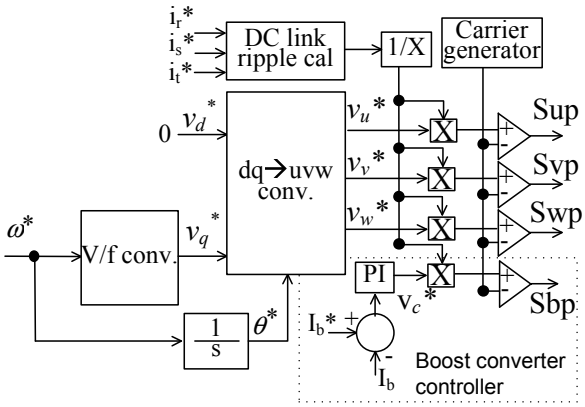

Fig. 4. Control block diagram.

In ref [2], this paper has been explained the boost converter is operating at every zero vector output of the inverter side. Fig. 5 illustrates about the current flow direction and the magnetic flux behaviour of a motor structure between the zero vector output and the non zero vector output.

The motor stucture in Fig. 5 is based on a standard three-phase 4-pole induction motor. The stator and the rotor are the electrical circuits that perform as electromagnets in an induction motor. For the stator winding, each group of coils surrounds the steel core to form an electromagnet. The rotor consists of a stack of steel laminations with evenly spaced conductor bars around the circumference. Phase windings are placed 30^0 apart in this example.

In Fig. 5(a) shows the positive-phase operating behaviour of an induction motor. Assuming the current is flowing at 60^0 intervals time, the output current i_u is zero current, i_v is a negative current and i_w is a positive current. As i_w flows into the stator, a magnetic flux will be formed from W1 to W3. Eventually, the rotor will be induced by the magnetic flux direction and rotates accordingly.

In Fig. 5(b) shows the zero-phase motor behaviour during the zero vector output, since the upper arm or the lower arm of the secondary side are all turned on together, no voltage flows across the motor. Battery current will take this period and flow into the leakage inductance (stator winding) thru the inverter switches and release out at the neutral point connection. Note that battery current flows into one direction only, and therefore magnetic flux cannot be produced.

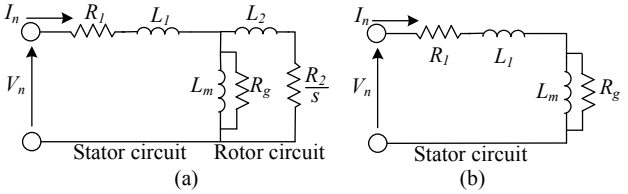

R_1=Stator resistor
L_1=Stator leakage inductance
R_2=Rotor resistor
L_2=Rotor leakage inductance
s = Slip
L_m=Magnetizing inductance
R_g= Magnetizing reactance

Fig. 6. Induction motor equivalent circuit. .

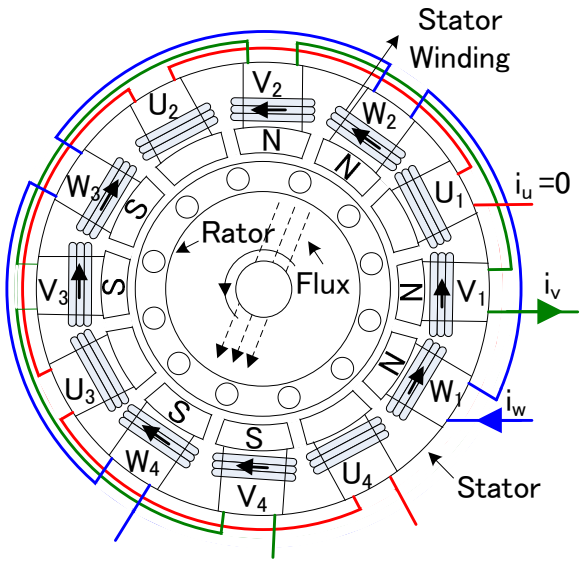

Fig. 5 (a). Positive-phase current flow diagram.

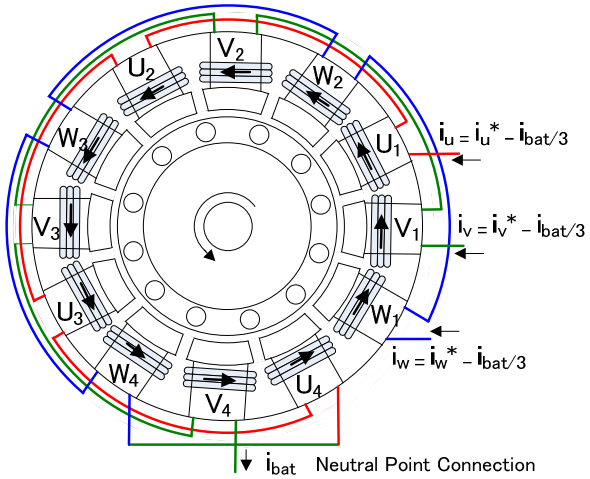

Fig. 5(b). Zero-phase current flow diagram.

Fig. 5. Induction motor interior structure.

Fig. 6(a) shows the induction motor equivalent and Fig. 6(b) shows the induction motor zero phase equivalent circuit. For the zero-phase, since there is no flux produced, the rotor circuit does not occur. Output current is derived as following,

$$I_n = I_n^* + i_{bat}/3 \quad . \tag{1}$$

where I_n = Positive phase motor current; n= u, v & w. i_{bat} = battery current;

The copper loss can be derived as following,

$$P_n = (I_n^{\,2} + \frac{1}{9} i_{bat}^{\,2}) R_1 \, . \tag{2}$$

Where P_n= Per-phase motor power loss;

IV. EXPERIMENTAL RESULTS

Table II shows the experiment parameters and the system connection is as described in Fig. 3. The conducted analyses are classified into three sections, the speed and torque curve, the torque impact characteristic and the acceleration and deceleration characteristic.

TABLE II. EXPERIMENT PARAMETERS

Input voltage	200 V	LC Filter Cut-off frequency	2.4 kHz
Input frequency	50 Hz	DC source	100 V
Carrier frequency	10 kHz	Measure leakage inductance	4.42 mH
Variable carrier frequency	20 kHz	Output frequency	10 Hz – 45 Hz

A. Speed and torque Curve

Fig. 7 shows the relations between the speed and torque characteristic of an induction motor. Fig. 7(a) shows the motoring data where only the indirect matrix converter is connected. Note that the V/f control is controlled at constant at all time. This graph shows a good control over an induction motor. The reason the speed is not constant to the torque is because induction motor consists of slip. The slip creates a difference in speed between the rotor and rotating magnetic field because no relative motion would exist if the two were turning at the same speed.

Fig. 7(b) shows the relations between speed and torque characteristic of the proposed circuit connected to an induction motor. The battery current was pre-set at 0 A when the torque is below than 20%. When the torque is larger than 20%, battery current will increase to 2 A. At 35 Hz output frequency, when the torque is 100%, the motor speed is 879 rpm. Likewise for the indirect matrix converter connection, under the same output frequency, when the torque is 100%, the motor speed is 877 rpm. The data in these two graphs show no difference, even the neutral point of the motor is connected to a boost converter. That is, the motor is running under a good operating condition.

B. Torque Impact

This section will demonstrate the torque impact characteristic under an EV mode and normal mode which is shown in Fig. 8. Fig. 8(a) shows the normal mode operation where the boost converter did not connect to the motor and only the indirect matrix converter is operating. The output frequency is 30 Hz, and the step increase of torque is 100%.

In Fig. 8(a), input current i_r shows an unbalanced sinusoidal waveform due to the low input power, where the input power is nearly 170 W. As the torque increases to 100%, input power immediately produces a larger power to maintain the speed. The output current i_u shows a good sinusoidal waveform at all the time.

The performance of a motor under the EV mode is shown in Fig. 8(b). The experimental condition is the same as in Fig. 8(a). The battery power is at 200 W at all the time, and the input power is nearly to 50W, therefore the i_r shows a bad quality of waveform due to low input power. When the torque increases to 100%, battery power maintains at 200 W and the input power eventually increases to keep the motor speed. The output current i_u demonstrates a good sinusoidal waveform at all the time which is the same as Fig. 8(a).

C. Acceleration and deaccleration characteristic

This section will demonstrate the speed characteristic of the proposed circuit under two different set-up conditions, normal mode and HEV mode. This experiment was conducted under a no-load condition. For the acceleration, the output frequency is increased from 10 Hz to 30 Hz. As for the deceleration, the output frequency is decreased from 30 Hz to 10 Hz.

Fig. 9(a) shows the indirect matrix converter only (normal mode) analysis data. During accelerating, large input power is required until the speed is at constant. Output current i_u shows a good sinusoidal waveform and change of frequency due to the accelerate and decelerate control.

Fig. 9(b) shows the proposed circuit speed characteristic data. When the motor is at low speed (f_{out}= 10Hz), the battery current is set at 0 A. Once the acceleration starts, the battery power increases to 200 W immediately. Therefore, during accelerating i_r shows a low current magnitude because battery power is used to drive the motor. When the speed is constant, battery power continues supplying and the input power drops.

Comparing between Fig. 9(a) and Fig. 9(b), it can be seen that the output current i_u is performing a good sinusoidal waveform. That is, the connection of neutral point of the motor for the used of a boost converter does not affect the performance of a motor. Furthermore, the results demonstrate a good control of batter power management is possible.

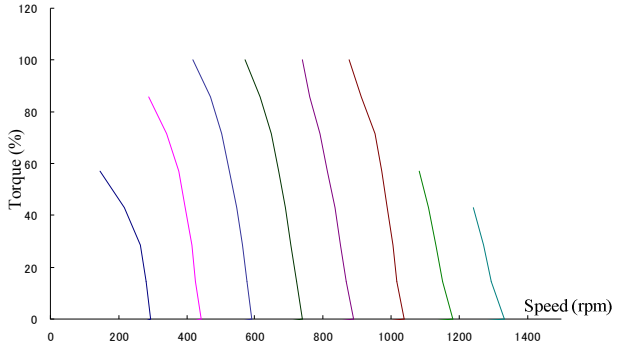

Fig. 7(a). Indirect matrix converter.

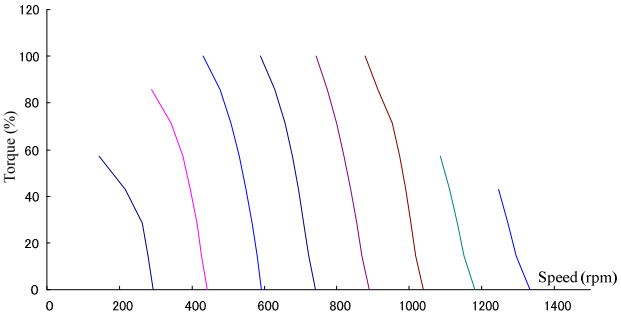

Fig. 7(b). Proposed circuit.

Fig. 7. Speed-torque characteristic analysis.

D. DC Link Voltage

This section will confirm the DC link voltage stability of the indirect matrix converter for another power source connection. In the proposed circuit, the DC link voltage is utilized to connect to an addition DC source. The battery energy will be released to the DC link part during the non zero vector output. The experimental results in Fig. 10 show that the battery voltage does not affect the DC link voltage of the indirect matrix converter.

Two conditions were verified in the experimental, mid speed region and high speed region. Figs. 10(a) and 10(b) show the experimental results where the motor speed is 475 rpm and the output power is 700W. In Fig. 10(a), the battery current is 0 A, and the DC link voltage is 270 V constantly. In Fig. 10(b), the battery current increases to 2 A, note that the DC link voltage can keep at constant even the input current magnitude has reduced.

The second condition is the high speed region where the motor speed is 900 rpm and the output power is 700W. Fig. 10(c) shows the result when the battery power is 0 W, and the DC link voltage is constantly at 270 V. Note that when the battery power increases to 200 W as shown in Fig. 10(d), the battery current contains of fluctuation but the DC link voltage still can maintain at constant. One of the reasons of the fluctuation is due to the tiny zero vector output cannot be formed due to the dead time error under high switching frequency. These results confirmed that the DC link voltage of the indirect matrix converter can be utilized and maintained by another DC power source.

V. Power Loss Experimental Measurement

Fig. 11 shows the proposed circuit experimental loss analysis data. The data (input power, battery power and output power) were directly taken from a power meter where the output power is controlled proportional to the load torque.

The symmetrical carrier and the asymmetrical carrier were applied one at a time to compare the losses of each method. The output frequency is 40 Hz, the output power is 750 W, and the battery power is 200W. Initially, the battery power does not supply, the battery power supplies when the output power is 300 W and above.

When the output power is low, the loss of the asymmetrical carrier is higher than the symmetrical carrier. One of the reasons is because when applying the asymmetrical method the input current contains of high harmonic component [10], this will cause the loss in LC filter increase. Furthermore, as the asymmetrical method has lesser zero output periods than the symmetrical method, eventually the conduction loss in primary side will increase.

When the output power is 300 W and above, the loss in chopper for the symmetrical method is 22 W and for the asymmetrical method is 15 W, respectively. This is because the sequence of zero vector output for the symmetrical method is more than the asymmetrical method. That is, the switching loss of the chopper is increased when symmetrical method applied.

Besides that, the asymmetrical method average produces switching frequency of 10 kHz per carrier time which will reduce the switching loss in the secondary side. On the other hand, the symmetrical method produces switching frequency of 20 kHz averagely. Therefore, most of the time, the loss of the symmetrical method is rather higher.

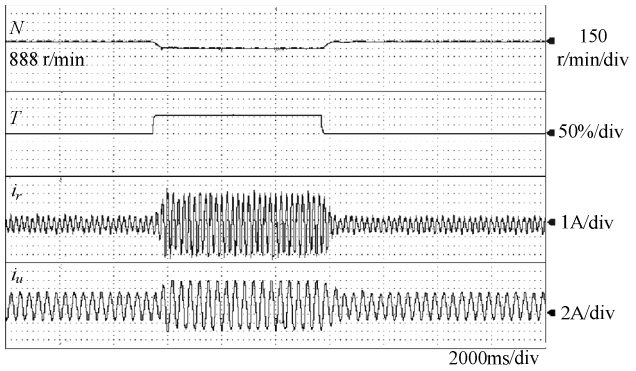

Fig. 8(a). Indirect matrix converter (normal mode).

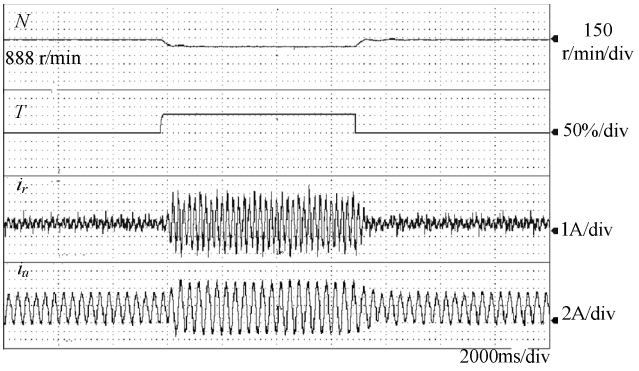

Fig. 8(b). Proposed circuit (EV mode).

Fig. 8. Torque Impact characteristic.

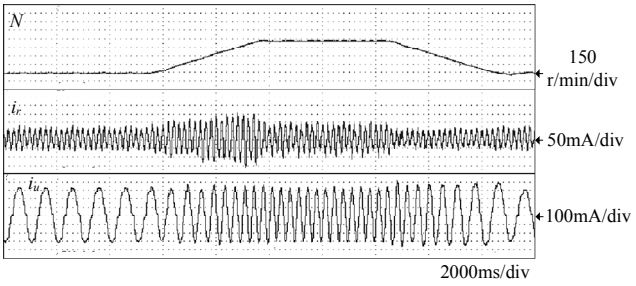

Fig. 9(a). Indirect matrix converter (normal mode).

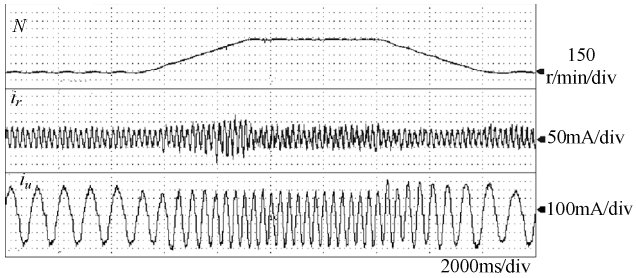

Fig. 9(b). Proposed circuit (HEV mode).

Fig. 9. Acceleration and Deceleration characteristic.

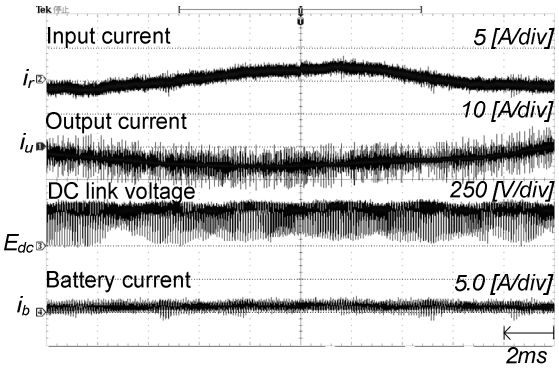

Fig. 10 (a). Mid speed region (Output frequency =20 Hz, i_{bat}=0 A).

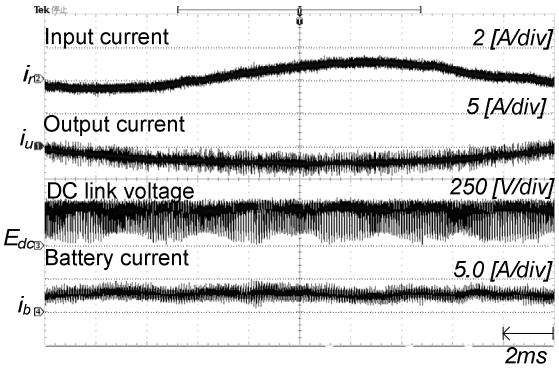

Fig. 10 (b). Mid speed region (Output frequency =20 Hz, i_{bat} =2 A).

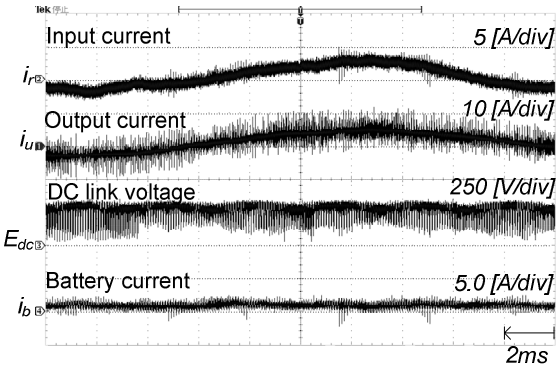

Fig. 10(c). High speed region (Output frequency =40 Hz, i_{bat} =0 A).

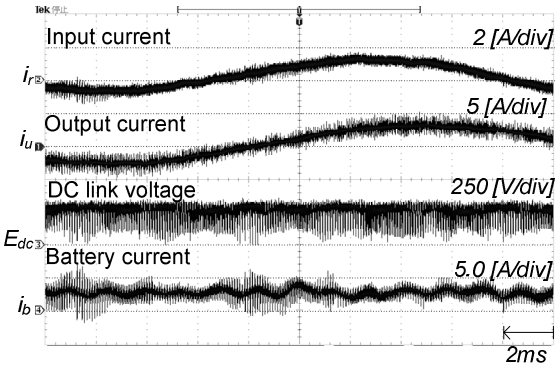

Fig. 10(d). High speed region (Output frequency =40 Hz, i_{bat} =2 A).

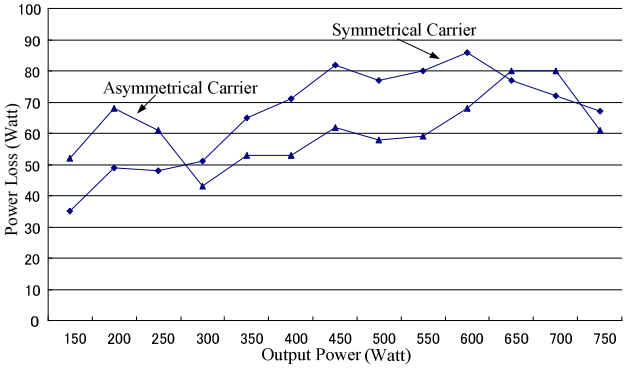

Fig. 11. Power loss experimental data

CONCLUSION

This paper discusses about the performance of an induction motor where the neutral point of the motor is connected to a DC boost converter. Several experimental test results have shown that the motor is under a good working condition even the stator leakage inductance is utilized to use in a boost converter operation. Besides, the DC link part of the indirect matrix converter is shown a stable connection point for an additional DC power source. Lastly, the total loss is shown to be 60 W±10% for a 750 W induction motor system.

REFERENCES

[1] Japan Automobile Manufacturers Association Inc, "Reducing CO2 Emissions in the Global Road Transport Sector", published 2008

[2] T.C Goh, and Jun-ichi Itoh, " A Three-Port Interface Converter by using an Indirect Matrix Converter with the Neutral Point of the Motor", in IEEE Energy Conversion Congress Expo, Sept 2009

[3] Kolar. J.W, Schafmeister. F, Round. S.D, and Ertl. H, "Novel Three-Phase AC-AC Sparse Matrix Converters", *IEEE Trans. Power Electronics*, Vol 22, pp. 1649-1661, Sept. 2007

[4] Jun-ichi Itoh, Sato. I, Odaka. A, Ohguchi. H, Kodachi. H, and Eguchi. N, "A Novel Approach to Practical Matrix Converter Motor Drive System with Reverse Blocking IGBT", *IEEE Trans. Power Electronics*, Vol 20, pp. 1356-1363, Nov. 2005

[5] Friedli. T, Heldwein. M.L, Giezendanner. F, and Kolar. J.W, "A High Efficiency Indirect Matrix Converter Utilizing RB-IGBTs", in *Power Electronics Specialist Conference*, pp. 1-7, June 2006

[6] Jun-ichi Itoh, and Tamura. H, "A novel Control Strategy for a Combined System using both Matrix Converter and Inverter without Interconnection Reactors", in *Power Electronics Specialist Conference*, pp. 1741-1747, June 2008

[7] Jun-ichi Itoh, Ikuya. S, Hideki. O, Kazuhisa. S, Akihiro. O, and Naoya. E, "A Control Method for The Matrix Converter based on virtual AC/DC/AC Conversion Using Carrier Comparison Method", *IEE Trans. in Japan*, Vol 152, pp. 65-73, Jun 2005

[8] Tsuji. M, Shuo Chen, Hamasaki. S, Xiaodan Zhao, and Yamada. E, "A Novel V/f control of induction motors for wide and precise speed operation", in SPEEDAM, pp.1130-1135, June 2008

[9] Chen Wei, Yang Rong Feng, Yu Yong, Wang Gao Lin, and Xu Dian Guo, "A novel Stability Improvement Method for V/f Controlled Induction Motor Drive Systems", In Electrical Machines and Systems 2008, pp.1073-1076, Oct 2008

[10] Jun-ichi Itoh, and Kato. K, "A Control Method of Indirect Matrix Converter for Reducing Switching Frequency", in JIASC, I-217, August 2008 (In Japanese)